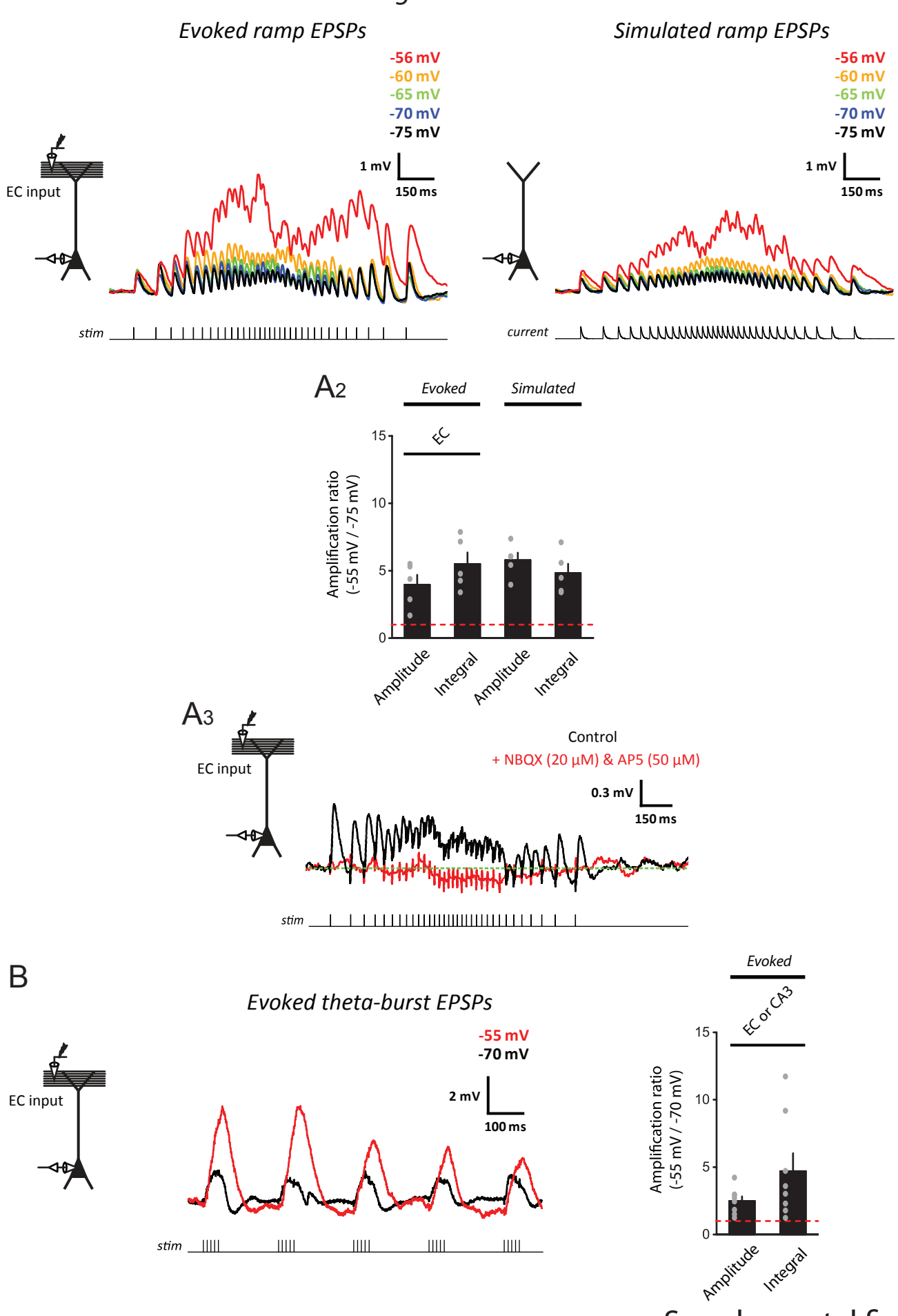

Supplemental figure 1

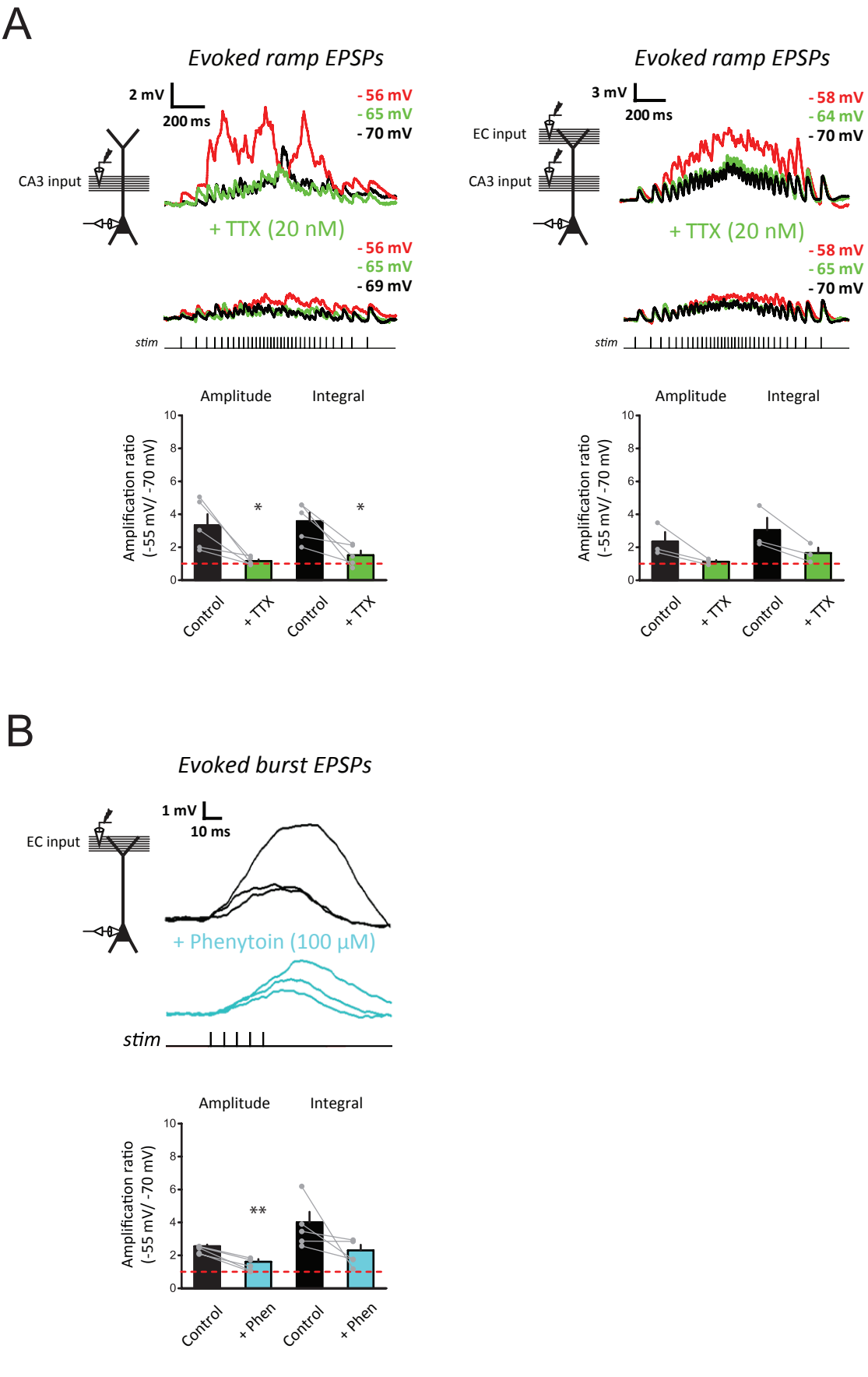

Supplemental figure 2

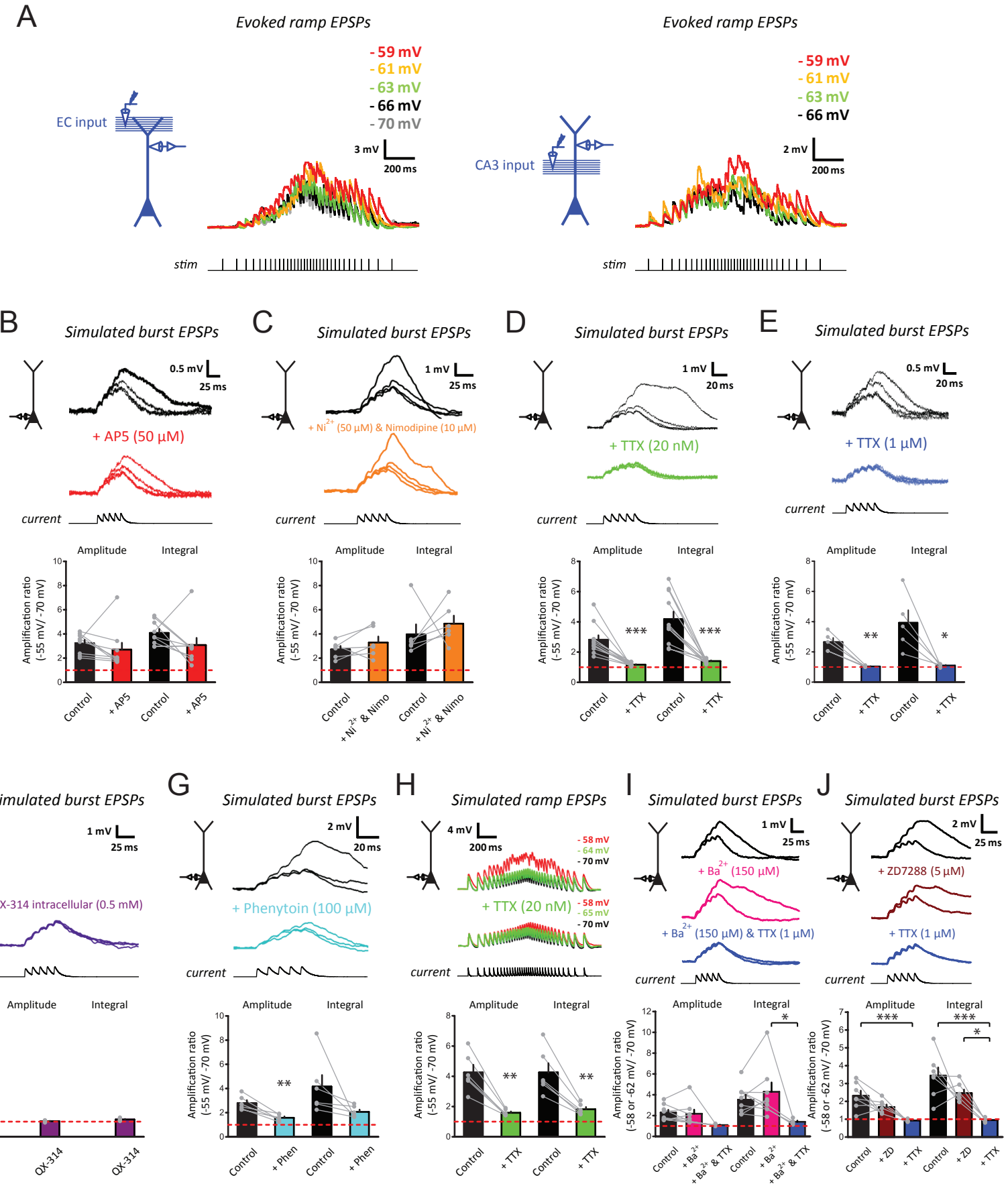

Supplemental figure 3

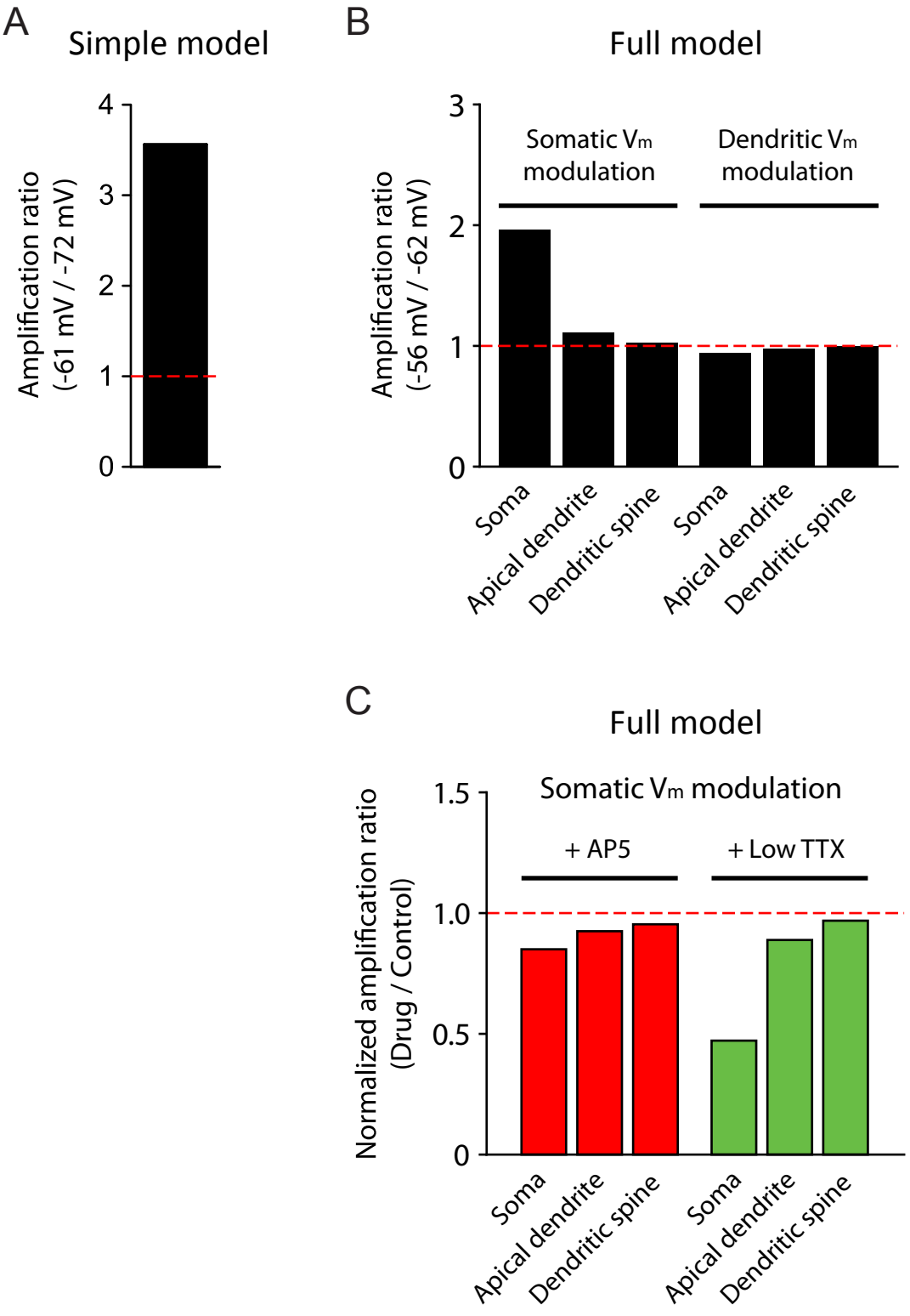

Supplemental figure 4

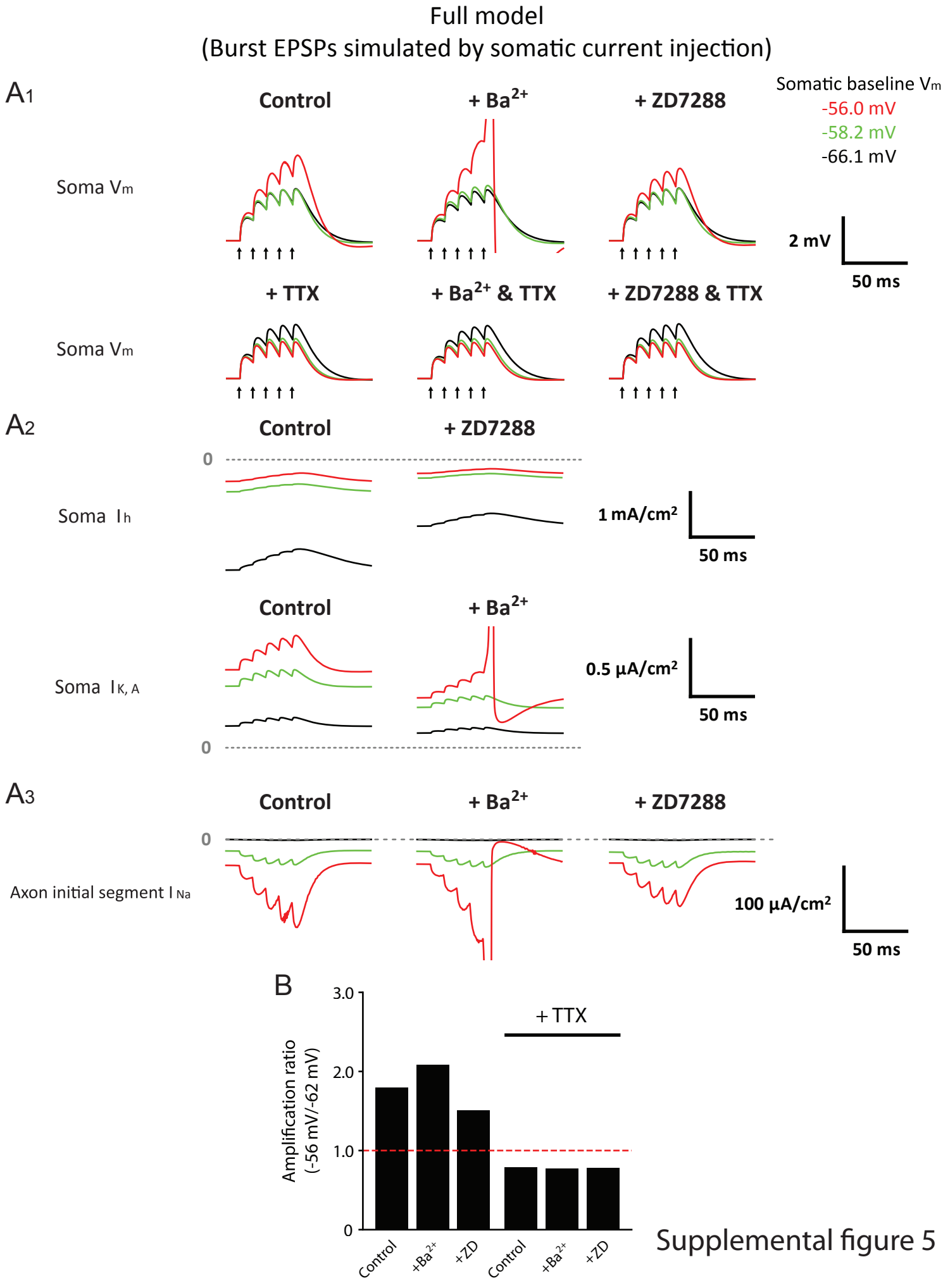

Supplemental figure 5

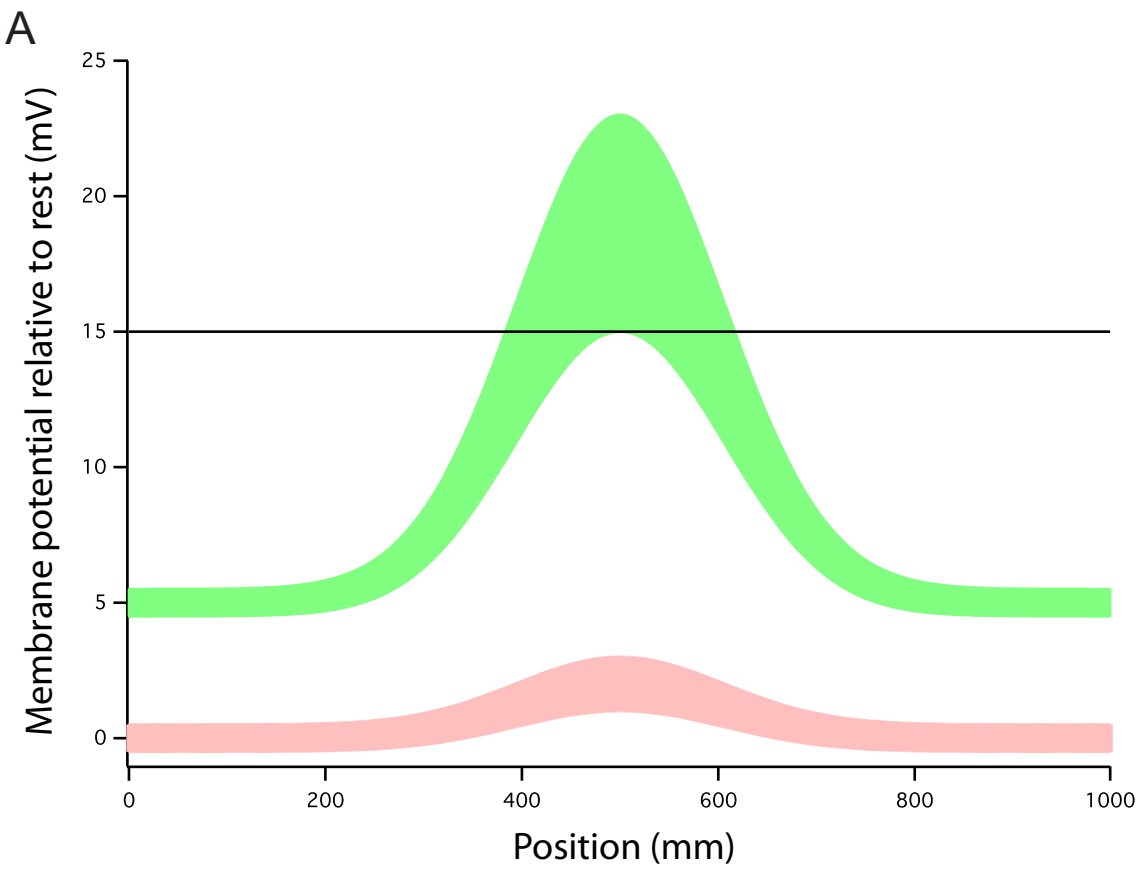

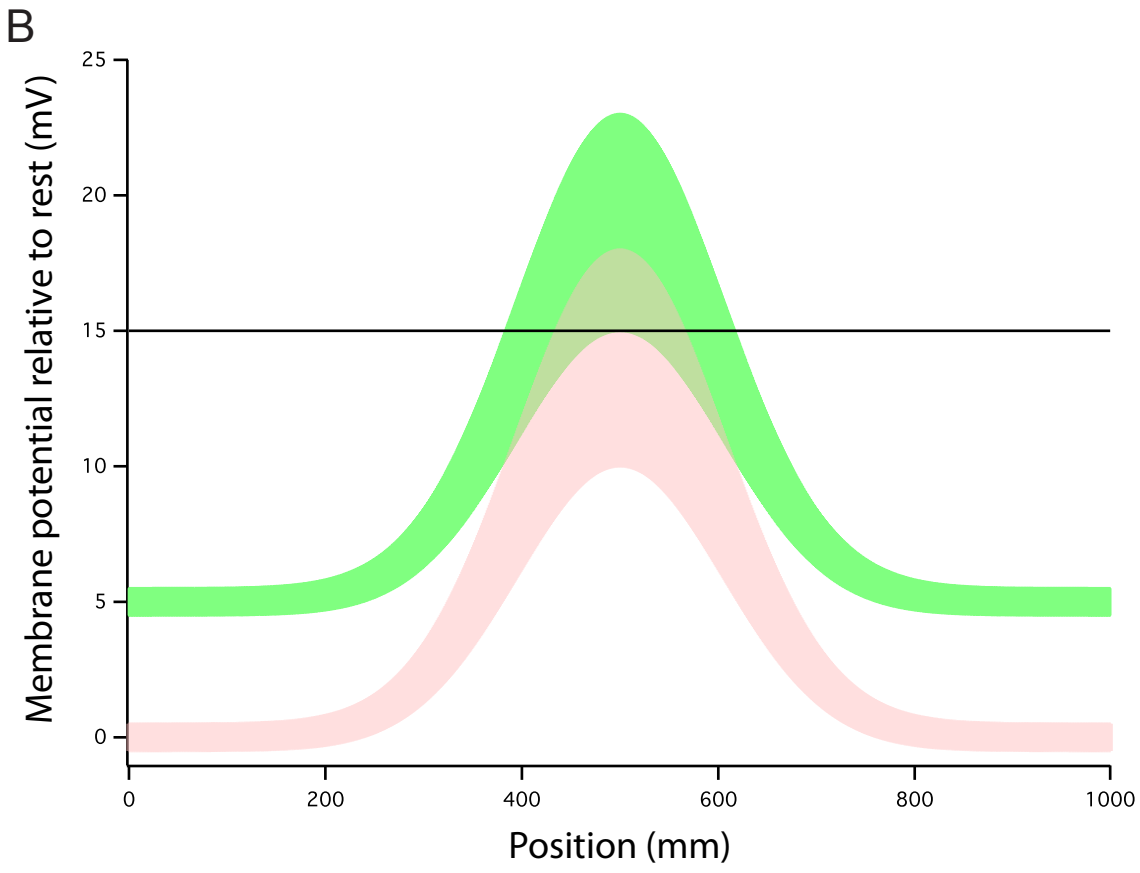

Supplemental figure 6

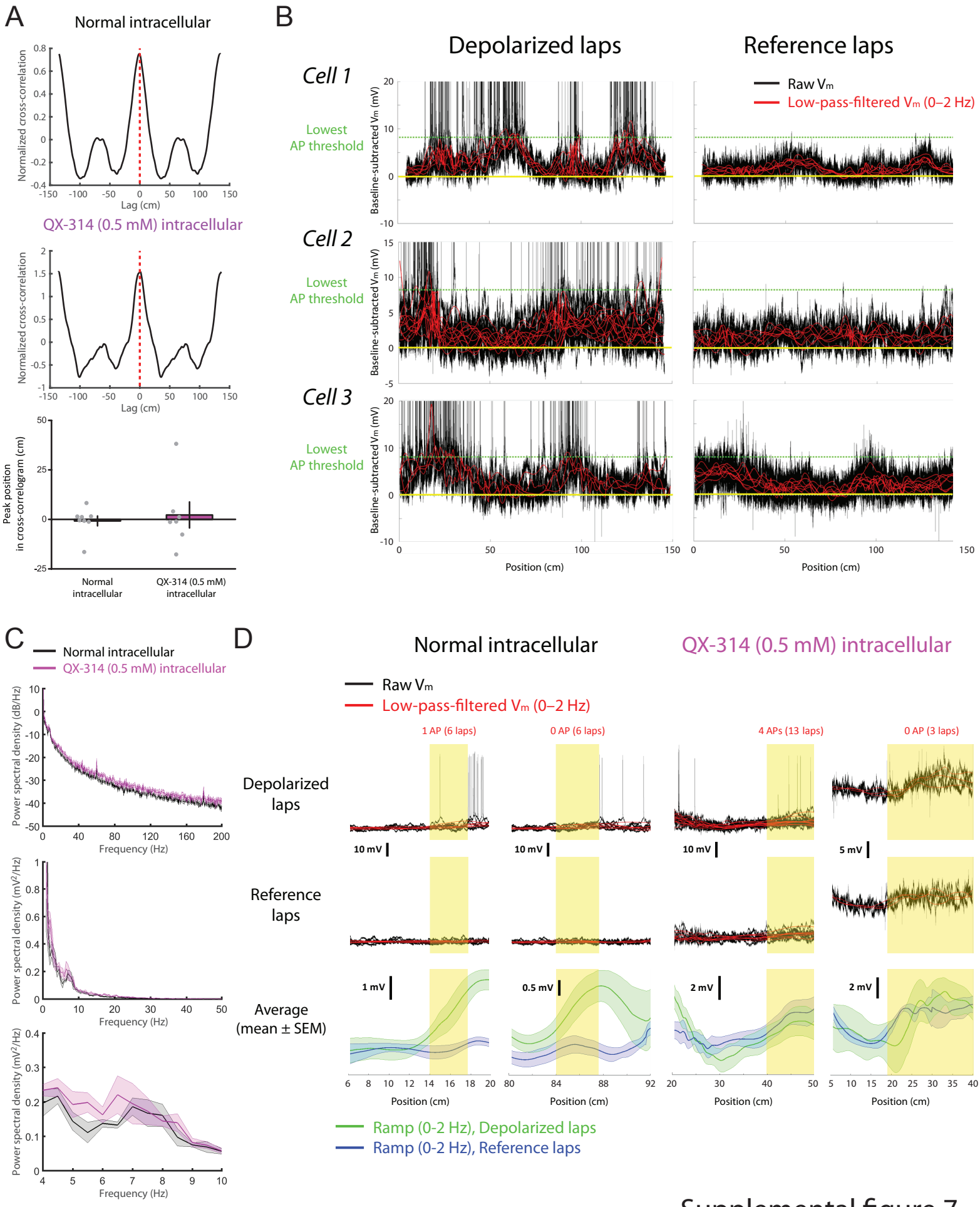

Supplemental figure 7

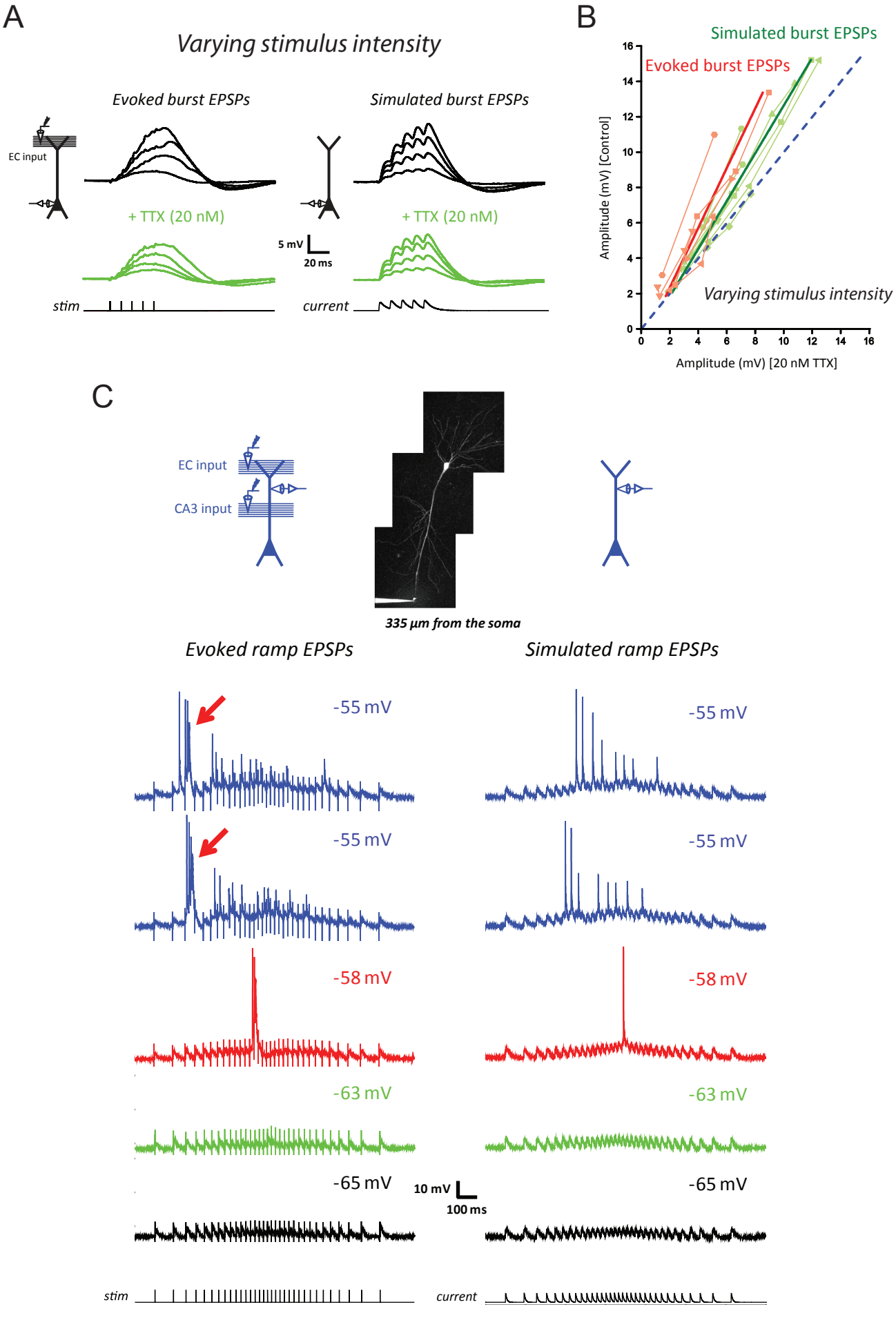

Supplemental figure 8

Supplemental Figure Legends

Figure S1. Temporally summated synaptic responses exhibit steep dependence on baseline membrane potential at the soma *in vitro* when responses are modulated at theta frequency or when GABAergic synaptic inhibition is intact. Related to Figure 1.

(A_1) Representative examples for voltage dependence of small, synaptically activated (*left*) and simulated (by injection of EPSC-like current waveform; *right*) responses at ramp-modulated frequency, with intact synaptic inhibition. Experimental configuration (*inset*) and representative traces of baseline-subtracted EPSPs at different baseline V_m (indicated at top-right).

(A_2) Summary of voltage-dependent amplification of synaptically activated and simulated responses at ramp-modulated frequency with intact synaptic inhibition (evoked, n = 5 neurons from 5 rats; simulated, n = 5 neurons from 5 rats). Dashed line indicates no amplification.

(A_3) Example of synaptically activated responses to a train of stimuli at ramp-modulated frequency in control, followed by application of 20 μM NBQX plus 50 μM AP5 via the bath, indicating that distal electrical stimulation (at least 650 μm away from the recorded neuron, see STAR Methods) used in these experiments (with intact synaptic inhibition) results in very limited direct activation of inhibitory interneurons.

(B) Voltage dependence of small, high-frequency burst EPSPs (5 stimuli at 100 Hz) modulated at a theta frequency (5 Hz). Experimental configuration (*inset*), representative traces of baseline-subtracted EPSPs at different baseline V_m (indicated at top-right; *left*), and summary of voltage-dependent amplification of synaptic responses (*right*; n = 8 neurons from 8 rats). Synaptic inhibition was blocked. Dashed line indicates no amplification.

EC, entorhinal cortex. Error bars indicate S.E.M..

Figure S2. A persistent, voltage-gated sodium current critically contributes to the steeply voltage-dependent amplification of temporally summated synaptic responses *in vitro*. Related to Figures 2–4.

(A) Voltage dependence of small, synaptically activated responses at ramp-modulated frequency in control, followed by application of 20 nM TTX (low TTX) via the bath. Experimental configuration (*inset*), representative traces of baseline-subtracted EPSPs at different baseline V_m (indicated at top-right; *top*), and summary of voltage-dependent amplification of synaptic responses in control and drug condition (*bottom*; CA3 input, n = 5 neurons from 5 rats; EC+CA3 inputs, n = 3 neurons from 3 rats). Dashed line indicates no amplification.

(B) As in (A), but for high-frequency synaptic activation (burst of 5 stimuli at 100 Hz) in control, followed by application of 100 µM phenytoin via the bath (n = 5 neurons from 5 rats).

EC, entorhinal cortex. *$p < 0.05$, **$p < 0.01$ by Student's t-test. Error bars indicate S.E.M..

Figure S3. A perisomatic voltage-gated sodium current critically contributes to the steeply voltage-dependent amplification of temporally summated synaptic responses *in vitro*. Related to Figures 2–4.

(A) Representative examples for voltage dependence of small, synaptically activated responses at ramp-modulated frequency in dendritic recordings. Experimental configuration (*insets*) and representative traces of baseline-subtracted EPSPs at different baseline V_m (indicated at top-right). Traces are from the same recording performed 198 µm from the soma. EC, entorhinal cortex.

(B) Voltage dependence of small, simulated (by injection of EPSC-like current waveform) burst EPSPs in somatic recordings in control, followed by application of 50 µM AP5 via the bath. Experimental configuration (*inset*), representative traces of baseline-subtracted EPSPs at different baseline V_m (*top*), and summary of voltage-dependent amplification of synaptic responses in control and drug condition (*bottom*; n = 9 neurons from 7 rats). Dashed line indicates no amplification.

(C) As in (B), but for bath application of 50 µM Ni^{2+} plus 10 µM nimodipine (n = 6 neurons from 4 rats).

(D) As in (B), but for bath application of low (20 nM) TTX (n = 11 neurons from 11 rats).

(E) As in (B), but for bath application of 1 μM TTX (n = 5 neurons from 5 rats).

(F) As in (B), but with 0.5 mM QX-314 (low QX-314) included in the intracellular solution (n = 6 neurons from 6 rats).

(G) As in (B), but for bath application of 100 μM phenytoin (n = 6 neurons from 6 rats).

(H) As in (B), but for responses at ramp-modulated frequency in somatic recordings in control, followed by application of low TTX via the bath (n = 6 neurons from 6 rats). Baseline V_m indicated at top-right.

(I) As in (B), but for bath application of 150 μM Ba^{2+} (n = 8 neurons from 7 rats), followed by 1 μM TTX (n = 5 neurons from 4 rats).

(J) As in (B), but for bath application and washout of 5 μM ZD7288 (to minimize the time-dependent off-target effects of ZD7288; n = 7 neurons from 4 rats), followed by bath application of 1 μM TTX (n = 5 neurons from 4 rats; see STAR Methods).

Voltage-dependent amplification was assessed at relatively less depolarized V_m to avoid continuous, pacemaker-like firing under the effects of Ba^{2+} or ZD7288 in (I) and (J) (see STAR Methods for details).

*p < 0.05, **p < 0.01, ***p < 0.001 by Student's t-test in (B)–(H) and one-way ANOVA with *post-hoc* means comparison using Tukey's test in (I) and (J). Error bars indicate S.E.M..

Figure S4. Perisomatic persistent sodium current critically contributes to the steeply voltage-dependent synaptic amplification *in silico*. Related to Figure 5.

(A) Summary of voltage-dependent amplification of small, high-frequency burst EPSPs (5 stimuli at 100 Hz) in the simple model (same as Figure 5A), showing amplification ratio based on the peak amplitude of synaptic responses.

(B) Summary of voltage-dependent amplification of small, high-frequency burst EPSPs (5 stimuli at 100 Hz) in somatic or dendritic recording in the full model of CA1 pyramidal neuron (same as Figure 5C), showing amplification ratio based on the peak amplitude of synaptic responses recorded from the soma, the apical dendritic trunk and a spine on the apical dendrites (250 µm from the soma). For dendritic V_m modulation (similar to the experiments in Figure 4E, F, S3A), *DC* current was injected to the apical dendritic trunk 250 µm from the soma (see STAR Methods for details of experimental design).

(C) Amplification ratio based on the peak amplitude of synaptic responses in different simulated drug conditions, normalized to the amplification ratio in control, for the simulations in Figure 5C.

Figure S5. Hyperpolarization-activated nonselective cation current and A-type voltage-dependent potassium current are not necessary for the steeply voltage-dependent synaptic amplification *in silico*. Related to Figures 5, S3 and S4.

(A) Voltage dependence of small, simulated (by injection of EPSC-like current waveform to the soma) burst EPSPs in the full model of CA1 pyramidal neuron (same as Figure 5C), with *DC* current injected to the soma to modulate V_m. Example traces of baseline-subtracted EPSPs recorded from the soma (A_1); instantaneous current through HCN channels (I_h) and A-type K_v channels ($I_{K,\,A}$) recorded from the soma (A_2); instantaneous current through Na_v channels (I_{Na}) recorded from the axon initial segment (A_3). Modeled voltages and currents were obtained from simulations performed at different somatic baseline V_m in control, simulated 150 µM Ba^{2+} (40% reduction in A-type K_v-channel conductance), simulated 5 µM ZD7288 (35% reduction in HCN-channel conductance), simulated 1 µM TTX (100% reduction in Na_v-channel conductance), or combinations of different simulated drug conditions. Note that in the example with Ba^{2+} (*top-middle* in (A_1)), a somatic action potential was triggered by the synaptic response at the most depolarized V_m. Arrows indicate timing of presynaptic input.

(B) Summary of voltage-dependent amplification of synaptic responses in control and different simulated drug conditions, showing amplification ratio based on the peak amplitude of synaptic responses. For the cases with Ba^{2+} and Ba^{2+} plus TTX, amplification ratio was measured using the peak amplitude during the 4^{th} EPSP due to the presence of the action potential.

Figure S6. Possible functional advantage of steeply voltage-dependent synaptic amplification. Related to Figure 6.

Schematic example of membrane potential relative to the resting membrane potential plotted as a function of the animal's position along a one-meter-long track. Black lines indicate the threshold for action potential firing. Gaussian functions were used to depict spatially modulated synaptic responses, with the variance consisting of a constant component (±0.5 mV) and a variable component (±0.5 mV at the peak of the response at the resting V_m, in the unscaled case) that has a linear dependence on the amplitude of the response as a function of position.

(A) In a scenario with steeply voltage-dependent synaptic amplification, spatially tuned synaptic responses at the resting V_m (red) were chosen to be small (average peak response, 2 mV), but amplified in response to a uniform depolarization of 5 mV (using an amplification factor of 7; green), thus causing all responses to cross the action potential threshold.

(B) In a scenario without steeply voltage-dependent synaptic amplification, in order to achieve a comparable level of firing in response to the same depolarization (green), spatially tuned synaptic responses at the resting V_m (red) had to be larger (same as green) and therefore falling closer to the threshold. This could result in threshold-crossing by some of the responses even in the absence of the uniform depolarization.

Figure S7. Strong voltage sensitivity of place-dependent firing *in vivo* is driven by voltage-dependent amplification of spatially tuned synaptic responses, primarily mediated by activation of a voltage-gated sodium current that is independent of somatic action potential firing. Related to Figure 7.

(A) Spatial coherence between ramp-like synaptic responses at different baseline membrane potentials. Representative examples of normalized cross-correlation between the average spatial profiles of baseline-subtracted, 0–2 Hz low-pass-filtered V_m during laps at relatively depolarized V_m (depolarized laps) and hyperpolarized V_m (reference laps) with normal (*top*) or low (0.5 mM) QX-314-containing (*middle*) intracellular solution. Dashed lines indicate the lag position where the maximum of cross-correlation occurred. Summary of spatial coherence between membrane potentials below somatic action potential threshold at different baseline V_m in the normal condition or with intracellular low QX-314 (*bottom*; normal, n = 8 neurons from 7 mice; intracellular low QX-314, n = 7 neurons from 7 mice). Error bars indicate S.E.M..

(B) Voltage dependence of relatively small spatially modulated synaptic ramps. Examples of baseline-subtracted, raw or 0–2 Hz low-pass-filtered V_m, plotted as a function of the animal's linearized position in the virtual environments during individual depolarized and reference laps. Green and yellow lines indicate the lowest apparent voltage threshold for all of the somatic action potentials for each recording and baseline V_m, respectively.

(C) Effects of intracellular low QX-314 on the frequency characteristics of membrane potential relevant for subthreshold synaptic responses. Estimates of power spectral density (PSD) on subthreshold V_m (in the absence of current injection) plotted on a logarithmic (*top*) or a linear scale (*middle* and *bottom*) for different frequency bands (see STAR Methods) in the normal condition or with intracellular low QX-314. For clarity, high power (at low frequencies) is not shown in two of the PSD plots (*top* and *middle*). Solid lines represent mean; shaded areas represent a relative error estimate for logarithmic representation (4.34*S.E.M./mean; *top*) and an absolute error estimate (S.E.M.; *middle* and *bottom*).

(D) Voltage dependence of spatially dependent synaptic ramps with a relatively small initial portion. Representative examples for the (individual or average) spatial profiles of raw or 0–2 Hz low-pass-filtered V_m for spatially modulated synaptic ramps (with the initial portion arising following an extended period of quiescence, i.e., ~3–10 seconds with no action potentials, and not large enough to drive significant firing at relatively depolarized V_m; see Results for details) during multiple depolarized and reference laps; data shown for the normal condition or with intracellular low QX-314, with two examples (as two columns) for each condition (from one mouse for the normal and two mice for the low-QX-314 condition). For recordings in different conditions (normal or intracellular low QX-314), synaptic ramps with matched conditions (see Results) were selected. Yellow shaded regions indicate initial portion, with the level of action potential (AP) firing in the corresponding region (during depolarized laps) labeled on the top.

Figure S8. Dendritic voltage-dependent amplification mechanisms are engaged at stronger levels of synaptic activation and dendritic depolarization. Related to Figure 8.

(A) Representative example for dependence of synaptically activated (*left*) and simulated (by injection of EPSC-like current waveform; *right*) burst EPSPs (in somatic recordings) on input strength (stimulus intensity or the amount of current injection) in control, followed by application of low (20 nM) TTX via the bath. Stimulus intensities used were relatively high, so the presynaptic effects of low TTX on synaptic transmission were negligible (see Results). Experimental configuration (*insets*) and representative traces of baseline-subtracted EPSPs in response to input with different strength.

(B) Summary of effects of low TTX on responses over a range of input strength, showing the peak amplitude of EPSPs in control plotted as a function of the peak amplitude of EPSPs in low TTX (evoked, n = 6 neurons from 6 rats; simulated, n = 8 neurons from 6 rats). Solid lines represent a linear fit to data points, and different symbols with a pale color denote data from different cells. Dashed line represents unity.

(C) Representative example for voltage dependence of synaptically activated (*left*) and simulated (*right*) dendritic responses at ramp-modulated frequency, tested at dendritic baseline V_m (indicated at top-right) covering a more depolarized range (than tested in Figure 4E, F, S3A, see Results for details of experimental design). Experimental configuration and Z-stack image of a dendritically recorded neuron (filled with 50 µM AF-594; *insets*). Arrows indicate dendritic plateau potentials. Recording was performed 335 µm from the soma.